

Exclusive heavy quarkonium + γ production from e^+e^- annihilation into a virtual photon

Hee Sok Chung, Jungil Lee, and Chaehyun Yu

Department of Physics, Korea University, Seoul 136-701, Korea

Abstract

We compute the cross section for exclusive production of a photon associated with a heavy quarkonium H of charge-conjugation parity $C = +1$ from e^+e^- annihilation into a virtual photon at the center-of-momentum energy $\sqrt{s} = 10.58$ GeV. The nonrelativistic QCD factorization formulas for the differential and total cross sections are obtained at leading order in the strong coupling and in the relative velocity of the heavy quark in the quarkonium rest frame. The predicted cross sections for the S -wave spin-singlet cases are about 80 fb and 50 fb for $H = \eta_c$ and $\eta_c(2S)$, respectively. Among P -wave spin-triplet charmonia, χ_{c1} has a particularly large cross section of about 14 fb. The cross sections for bottomonium states η_b and χ_{bJ} are about 3 fb. A rough estimate of the background reveals that the signal significances for charmonium processes are sufficiently large enough to be detected with ease with the integrated luminosities available at the present B factories.

PACS numbers: 12.38.-t, 12.39.St, 13.66.Bc, 14.40.Gx

I. INTRODUCTION

The measurements of the cross section for exclusive $J/\psi + \eta_c$ production from e^+e^- annihilation carried out by the Belle [1, 2] and BABAR [3] collaborations have triggered rapid progress in the heavy-quarkonium theory based on the nonrelativistic QCD (NRQCD) factorization approach [4]. The original empirical cross section in Ref. [1] was greater than the theoretical predictions by Braaten and Lee [5] and by Liu, He, and Chao [6] by an order of magnitude. Scenarios that the signal may contain other final states like $J/\psi + J/\psi$ [7, 8] or J/ψ +glueball [9] were ruled out by an updated Belle analysis [2]. There was an argument that an appropriate choice of the light-cone wave function [10] may enhance the theoretical prediction significantly, which was disfavored by a following study [11]. Zhang, Gao, and Chao reported large corrections of next-to-leading order in the strong coupling α_s [12] and the result was confirmed by Gong and Wang [13], but the corrections were not large enough to resolve the discrepancy between experiment and theory. In the mean time, Bodwin, Kang, and Lee introduced a new method of resumming relativistic corrections of a class of color-singlet contributions to all orders in v [14], where v is the relative velocity of the heavy quark or antiquark in the meson rest frame. The method was applied to compute the relativistic corrections to $e^+e^- \rightarrow J/\psi + \eta_c$ [15]. Finally, Bodwin, Lee, and Yu reported that the discrepancy had been resolved within errors [16], after including both the resummed relativistic corrections and next-to-leading order QCD corrections by Zhang, Gao, and Chao. In addition, the first proof of the factorization theorem for exclusive charmonium production in B decay and exclusive two-charmonium production from e^+e^- annihilation to all orders in perturbation theory in QCD was presented very recently by Bodwin, Garcia i Tormo, and Lee [17].

As shown in Ref. [5], at leading order in v , a non-negligible amount of the cross section for the exclusive production of charge-conjugation parity $C = +1$ charmonium (H) associated with a J/ψ from e^+e^- annihilation into a virtual photon comes from the interference between QCD and QED subprocesses, where the QED subprocess involves $\gamma^* \rightarrow H + \gamma^*$ followed by the photon fragmentation $\gamma^* \rightarrow J/\psi$. The interference contributions are about +30%, +5%, -6%, and 10% for $H = \eta_c, \chi_{c0}, \chi_{c1},$ and χ_{c2} , respectively [5]. This means that the pure QED contributions are about 10%, 0.3%, 0.4%, and 1% of the total cross sections, respectively. We notice that, in comparison with the QED subprocess for $e^+e^- \rightarrow H + J/\psi$, the rate for

$e^+e^- \rightarrow H + \gamma$ is enhanced by a scaling factor of $1/(\alpha v^3) \sim 10^3$ for a charmonium, where α is the QED coupling. Based on this rough estimate, we expect that the cross section for $e^+e^- \rightarrow H + \gamma$ can be greater than that for $e^+e^- \rightarrow H + J/\psi$ by 2 orders of magnitude for $H = \eta_c$. For the P -wave spin-triplet charmonia, the enhancement factors range from about 1 to 10. Therefore, as long as the severe background from $e^+e^- \rightarrow X + \gamma$ is well controlled in the recoil mass (m_X) regions near the H resonances, the processes $e^+e^- \rightarrow H + \gamma$ can be detected by analyzing the photon energy spectrum in $e^+e^- \rightarrow X + \gamma$.

In this paper, we compute the cross section for the exclusive process $e^+e^- \rightarrow H + \gamma$ at the center-of-momentum (CM) energy $\sqrt{s} = 10.58$ GeV, where H is a heavy quarkonium of charge-conjugation parity $C = +1$. We consider S -wave spin-singlet states η_c , $\eta_c(2S)$, and η_b and P -wave spin-triplet states χ_{cJ} and χ_{bJ} , where $J = 0, 1$, and 2 .¹ Perturbative calculation is carried out at order $\alpha^3\alpha_s^0$ and at leading order in v . The remainder of this paper is organized as follows. In Sec. II, we compute the short-distance coefficients for the NRQCD factorization formulas for the $e^+e^- \rightarrow H + \gamma$ cross sections. The numerical values for the input parameters such as long-distance NRQCD matrix elements are given in Sec. III. The cross sections for $e^+e^- \rightarrow H + \gamma$ at the B factories are predicted in Sec. IV, where a rough estimate on the background is also given. Then, we summarize our results in Sec. V.

II. PERTURBATIVE CALCULATION

In this section, we derive the NRQCD factorization formula for the exclusive process $e^+e^- \rightarrow H + \gamma$ at leading order in both α_s and v , where H is a heavy quarkonium of charge-conjugation parity $C = +1$. The quarkonia H that we consider in this paper are the S -wave spin-singlet (1S_0) state, η_Q , and the P -wave spin-triplet (3P_J) states, χ_{QJ} , for $J = 0, 1$, and 2 , where the heavy quark Q is the charm or the bottom quark. Because the C parity of the final state is -1 , at leading order in α , an exclusive $H + \gamma$ final state can be produced from e^+e^- annihilation into a virtual photon. A heavy quarkonium with $C = -1$ can be produced associated with a photon from e^+e^- annihilation into two photons, which we do not consider here.

¹ Throughout this paper we suppress the identifier ($1P$) for any $1P$ quarkonium.

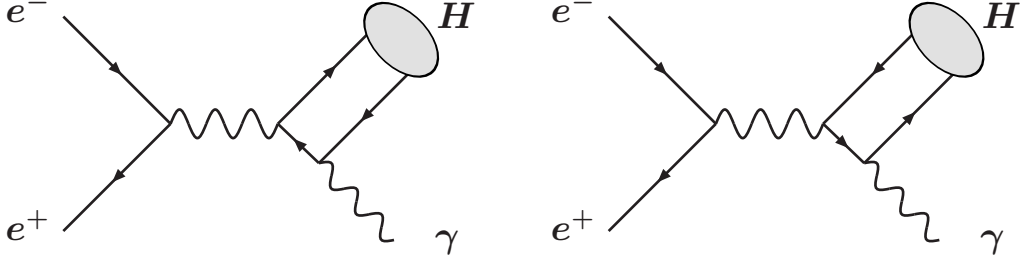


FIG. 1: Feynman diagrams for the exclusive production of a $C = +1$ heavy quarkonium associated with a photon from e^+e^- annihilation into a virtual photon at leading order in α and α_s .

A. Amplitude

The Feynman diagrams for the exclusive process $e^+(k_2) e^-(k_1) \rightarrow H(P, \lambda_H) + \gamma(k, \lambda)$ at order $\alpha^3 \alpha_s^0$ are shown in Fig. 1. Here, k_1 , k_2 , P , and k are the momenta for the e^- , e^+ , H , and γ , respectively. The helicities of the H and γ are denoted by λ_H and λ , respectively. The S -matrix element for the process is given by

$$-i\mathcal{M}_H(\lambda_H, \lambda) = -i\frac{e}{s} L_\mu \mathcal{A}_H^{\mu\nu}(\lambda_H) \epsilon_{\gamma\nu}^*(\lambda), \quad (1)$$

where $-e$ is the electric charge of the electron and ϵ_γ is the polarization four-vector of the photon. The leptonic current L_μ in Eq. (1) is defined by

$$L_\mu = \bar{v}(k_2) \gamma_\mu u(k_1). \quad (2)$$

The factor $\mathcal{A}_H^{\mu\nu} \epsilon_{\gamma\nu}^*$ in Eq. (1) corresponds to the amplitude for $\gamma^*(Q) \rightarrow H(P, \lambda_H) + \gamma(k, \lambda)$, where Q is the momentum of the virtual photon γ^* .

B. Effective vertex

$\mathcal{A}_H^{\mu\nu}$ in Eq. (1) contains nonperturbative contributions of the $Q\bar{Q}$ pair that evolves into the heavy quarkonium H . In the NRQCD factorization approach [4], the hadronic tensor $\mathcal{A}_H^{\mu\nu}$ can be expanded as a linear combination of NRQCD matrix elements that involve the long-distance nature of the $Q\bar{Q}$ pair. A corresponding short-distance coefficient of each NRQCD matrix element is insensitive to the long-distance nature of the pair and calculable perturbatively. According to the velocity scaling rules of NRQCD, NRQCD matrix elements are classified in powers of v [4]. Thus, the expansion can be truncated at a given order of

accuracy. The velocity scaling factor of an NRQCD matrix element is determined by the spectroscopic state of the $Q\bar{Q}$ pair, $[Q\bar{Q}]_1^{(2s+1)L_J}$, and that of the H into which the $Q\bar{Q}$ pair evolves. Here, s , L , and J are the spin, orbital angular momentum, and total angular momentum of the $Q\bar{Q}$ pair, respectively, and the subscript 1 indicates that the pair is in a color-singlet state.

For the exclusive process $\gamma^* \rightarrow H + \gamma$, the color-singlet $Q\bar{Q}$ pair with the spectroscopic state identical to that of the H contributes at leading order in v . In order to determine the corresponding short-distance coefficient, we compute the $Q\bar{Q}$ analog $\mathcal{A}_Q^{\mu\nu}$ of the hadronic tensor $\mathcal{A}_H^{\mu\nu}$, where $\mathcal{A}_Q^{\mu\nu(2s+1)L_J}\epsilon_{\gamma\nu}^*$ is the amplitude for the perturbative process $\gamma^*(Q) \rightarrow [Q(p)\bar{Q}(\bar{p})]_1^{(2s+1)L_J} + \gamma(k)$. Here, the four-momenta p and \bar{p} for the Q and the \bar{Q} , respectively, can be expressed in terms of the total momentum P and half their relative momentum q :

$$p = \frac{1}{2}P + q, \quad (3a)$$

$$\bar{p} = \frac{1}{2}P - q, \quad (3b)$$

where $P \cdot q = 0$. In the $Q\bar{Q}$ rest frame, $P = (2E, \mathbf{0})$, $q = (0, \mathbf{q})$, $E = (m^2 + \mathbf{q}^2)^{1/2}$, and m is the mass of the heavy quark Q . At leading order in v , P can be identified as the quarkonium momentum. The amplitude for the perturbative process $\gamma^*(Q) \rightarrow Q(p)\bar{Q}(\bar{p}) + \gamma(k, \lambda)$ is given by

$$\mathcal{M}^\mu[\gamma^*(Q) \rightarrow Q(p)\bar{Q}(\bar{p}) + \gamma(k, \lambda)] = \bar{u}(p)\mathcal{A}^{\mu\nu}v(\bar{p})\epsilon_{\gamma\nu}^*(\lambda). \quad (4)$$

The tensor $\mathcal{A}^{\mu\nu}$ in Eq. (4) is defined by

$$\mathcal{A}^{\mu\nu} = e_Q^2 e^2 [\gamma^\mu \Lambda(-\bar{p} - k)\gamma^\nu + \gamma^\nu \Lambda(p + k)\gamma^\mu] \otimes \mathbb{1}, \quad (5)$$

where e_Q is the fractional electric charge of the heavy quark Q , $\Lambda(p) = (\not{p} + m)/(p^2 - m^2)$, and $\mathbb{1}$ is the unit matrix of the color $SU(N_c)$ for $N_c = 3$.

$\mathcal{A}^{\mu\nu}$ in Eq. (4) may contain various $[Q(p)\bar{Q}(\bar{p})]_1^{(2s+1)L_J}$ contributions. The $Q\bar{Q}$ analog $\mathcal{A}_Q^{\mu\nu(2s+1)L_J}$ of the hadronic tensor can be obtained from $\mathcal{A}^{\mu\nu}$ in Eq. (5) by restricting the $Q\bar{Q}$ pair to have an appropriate spectroscopic state. A given spin state of the color-singlet $Q\bar{Q}$ pair can be projected out from Eq. (4) by replacing the outer product $v(\bar{p})\bar{u}(p)$ with the corresponding spin projector given in Ref. [18]. The color-singlet spin-singlet projector is denoted by Π_1 and the color-singlet spin-triplet projector is by $\Pi_3^\mu \epsilon_\mu^*(\lambda_s)$, where $\epsilon(\lambda_s)$ is

the polarization for the spin-triplet state with the helicity λ_s . Expressions for the Π_1 and Π_3^μ are given by [18]

$$\Pi_1 = \frac{(\not{p} - m)\gamma^5(\not{P} + 2E)(\not{p} + m)}{4\sqrt{2}E(E + m)} \otimes \frac{1}{\sqrt{N_c}} \mathbb{1}, \quad (6a)$$

$$\Pi_3^\mu = -\frac{(\not{p} - m)\gamma^\mu(\not{P} + 2E)(\not{p} + m)}{4\sqrt{2}E(E + m)} \otimes \frac{1}{\sqrt{N_c}} \mathbb{1}. \quad (6b)$$

We still need to project out an appropriate orbital-angular-momentum state. In order to project out the S -wave contribution at leading order in v , one must put $q = 0$. By making use of Eqs. (5) and (6a), we obtain the $Q\bar{Q}$ analog $\mathcal{A}_Q^{\mu\nu}(^1S_0)$ of the hadronic tensor for the S -wave color-singlet spin-singlet state:

$$\mathcal{A}_Q^{\mu\nu}(^1S_0) = \text{Tr}[\mathcal{A}^{\mu\nu}\Pi_1] \Big|_{q=0}, \quad (7)$$

where the trace is over both spin and color indices.

The P -wave contribution at leading order in v is proportional to the first derivative of Eq. (4) with respect to q . By making use of Eqs. (5) and (6b), we obtain the $Q\bar{Q}$ analog $\epsilon_\rho^*(\lambda_s)\epsilon_\tau^*(\lambda_\ell)\mathcal{A}_Q^{\mu\nu\rho\tau}$ of the hadronic tensor for the P -wave color-singlet spin-triplet state, where $\epsilon(\lambda_\ell)$ is the polarization for the P -wave orbital-angular-momentum state and

$$\mathcal{A}_Q^{\mu\nu\rho\tau} = \frac{\partial}{\partial q_\rho} \text{Tr}[\mathcal{A}^{\mu\nu}\Pi_3^\tau] \Big|_{q=0}. \quad (8)$$

Like Eq. (7) the trace in Eq. (8) is over both spin and color indices. The $Q\bar{Q}$ analog $\mathcal{A}_Q^{\mu\nu}(^3P_J, \lambda_H)$ of the hadronic tensor for the $[Q\bar{Q}]_1(^3P_J)$ for $J = 0, 1$, and 2 can be read off by projecting out the diagonal, antisymmetric, and symmetric traceless components with respect to the vector indices for s and L [5]:

$$\mathcal{A}_Q^{\mu\nu}(^3P_0) = \mathcal{A}_Q^{\mu\nu\rho\tau} \frac{1}{\sqrt{3}} I_{\rho\tau}, \quad (9a)$$

$$\mathcal{A}_Q^{\mu\nu}(^3P_1, \lambda_H) = \mathcal{A}_Q^{\mu\nu\rho\tau} \frac{i}{2E\sqrt{2}} \epsilon_{\rho\tau\alpha\beta} P^\alpha \epsilon_H^{*\beta}(\lambda_H), \quad (9b)$$

$$\mathcal{A}_Q^{\mu\nu}(^3P_2, \lambda_H) = \mathcal{A}_Q^{\mu\nu\rho\tau} \epsilon_{H\rho\tau}^*(\lambda_H), \quad (9c)$$

where λ_H is the helicity of H . ϵ_H^β in Eq. (9b) and $\epsilon_H^{\alpha\beta}$ in Eq. (9c) are the spin-1 polarization vector for the $[Q\bar{Q}]_1(^3P_1)$ pair and the spin-2 polarization tensor for the $[Q\bar{Q}]_1(^3P_2)$ pair, respectively. Note that $\epsilon_H^{\alpha\beta} = \epsilon_H^{\beta\alpha}$ and $\epsilon_H^\alpha{}_\alpha = 0$. Because we consider the color-singlet contributions at leading order in v , the polarization vector and tensor are treated to be

identical to those for $H(^3P_1)$ and $H(^3P_2)$, respectively. The tensor $I_{\mu\nu}$ appearing in Eq. (9) is defined by

$$I_{\mu\nu} = -g_{\mu\nu} + \frac{P_\mu P_\nu}{(2E)^2}. \quad (10)$$

As a result, we obtain the effective vertex for the perturbative process $\gamma^* \rightarrow [Q\bar{Q}]_1(^{2s+1}L_J) + \gamma$ as

$$\mathcal{A}_Q^{\mu\nu}(^1S_0) = -\frac{4\sqrt{6}e_Q^2 e^2}{Q^2 - P^2} \epsilon^{\mu\nu\alpha\beta} P_\alpha Q_\beta, \quad (11a)$$

$$\mathcal{A}_Q^{\mu\nu}(^3P_0) = i \frac{8\sqrt{2}e_Q^2 e^2 (Q^2 - 3P^2)}{\sqrt{P^2}(Q^2 - P^2)^2} \left[\frac{1}{2}(Q^2 - P^2)g^{\mu\nu} + P^\mu P^\nu \right], \quad (11b)$$

$$\mathcal{A}_Q^{\mu\nu}(^3P_1) = \frac{16\sqrt{3}e_Q^2 e^2 Q^2 \epsilon_{H\sigma}^*(\lambda_H)}{P^2(Q^2 - P^2)^2} \left[P^\mu P_\alpha Q_\beta \epsilon^{\nu\alpha\beta\sigma} - P^\nu P_\alpha Q_\beta \epsilon^{\mu\alpha\beta\sigma} - \frac{1}{2}(Q^2 - P^2)P_\alpha \epsilon^{\mu\nu\alpha\sigma} \right], \quad (11c)$$

$$\begin{aligned} \mathcal{A}_Q^{\mu\nu}(^3P_2) = i \frac{16\sqrt{6}e_Q^2 e^2 \sqrt{P^2} \epsilon_{H\alpha\beta}^*(\lambda_H)}{(Q^2 - P^2)^2} & \left[g^{\mu\nu} Q^\alpha Q^\beta + P^\mu Q^\alpha g^{\nu\beta} - P^\nu Q^\alpha g^{\mu\beta} \right. \\ & \left. + \frac{1}{2}(Q^2 - P^2)g^{\mu\alpha} g^{\nu\beta} \right]. \end{aligned} \quad (11d)$$

In the limit $Q^2 \rightarrow 0$, the expressions in Eq. (11) reduce into the effective vertices for the decay $[Q\bar{Q}]_1(^{2s+1}L_J) \rightarrow \gamma\gamma$. We observe that the vertex for 3P_1 in Eq. (11c) is proportional to Q^2 . Because of this reason, $\gamma^* \rightarrow [Q\bar{Q}]_1(^3P_1) + \gamma$ is not forbidden while the amplitude for $[Q\bar{Q}]_1(^3P_1) \rightarrow \gamma\gamma$ vanishes.

C. Perturbative matching

The $Q\bar{Q}$ analogs $\mathcal{A}_Q^{\mu\nu}(^{2s+1}L_J)$ (11) for the hadronic tensors contain perturbative NRQCD matrix elements. At the squared amplitude level, those perturbative NRQCD matrix elements at the leading order in v are $\langle 0 | \mathcal{O}_1^{[Q\bar{Q}]_1(^{2s+1}L_J)}(^{2s+1}L_J) | 0 \rangle$ for the color-singlet $^{2s+1}L_J$ state, where \mathcal{O}_1 is the local four-quark operator of NRQCD [4]. In general, the production matrix elements are related to the NRQCD matrix elements for the decay under vacuum-saturation approximation, which is valid up to corrections of relative order v^4 [4]. For exclusive production through the electromagnetic interaction, the v -leading perturbative NRQCD matrix elements for the 1S_0 and 3P_J states are simply expressed at the amplitude

level as

$$\langle [Q\bar{Q}]_1(^1S_0)|\psi^\dagger\chi|0\rangle = 2E\sqrt{2N_c}, \quad (12a)$$

$$\frac{1}{\sqrt{3}}\langle [Q\bar{Q}]_1(^3P_0)|\psi^\dagger\left(-\frac{i}{2}\overleftrightarrow{\mathbf{D}}\cdot\boldsymbol{\sigma}\right)\chi|0\rangle = 2E\sqrt{2N_c}|\mathbf{q}|, \quad (12b)$$

$$\frac{1}{\sqrt{2}}\langle [Q\bar{Q}]_1(^3P_1)|\psi^\dagger\left(-\frac{i}{2}\overleftrightarrow{\mathbf{D}}\times\boldsymbol{\sigma}\cdot\boldsymbol{\epsilon}_H\right)\chi|0\rangle = 2E\sqrt{2N_c}|\mathbf{q}|, \quad (12c)$$

$$\sum_{ij}\langle [Q\bar{Q}]_1(^3P_2)|\psi^\dagger\left(-\frac{i}{2}\overleftrightarrow{D}^{(i}\sigma^j)\epsilon_H^{ij}\right)\chi|0\rangle = 2E\sqrt{2N_c}|\mathbf{q}|, \quad (12d)$$

where ψ^\dagger and χ are two-component Pauli spinors creating a heavy quark and a heavy antiquark, respectively, σ^i is a Pauli matrix, and \mathbf{D} is the spatial part of the gauge covariant derivative. Note that only a single polarization state is projected out in the expressions in Eqs. (12c) and (12d). In Eq. (12d), the following notation for the symmetric traceless component of a tensor is used: $A^{(ij)} = \frac{1}{2}(A^{ij} + A^{ji}) - \frac{1}{3}\delta^{ij}\sum_k A^{kk}$. The factors of $2E$ appear on the right sides of Eq. (12), because the state $|[Q\bar{Q}]_1(^{2s+1}L_J)\rangle$ on the left sides is normalized relativistically. In Eq. (8), we have taken the derivative with respect to q . Therefore, when we read the corresponding short-distance coefficients, we must cancel the overall factor $|\mathbf{q}|$ in Eqs. (12b), (12c), and (12d). Replacement of the gauge covariant derivative \mathbf{D} by an ordinary derivative ∇ brings in corrections of relative order v^2 in the Coulomb gauge [4] in which the NRQCD operators are defined.

By making use of Eqs. (7), (9), and (12), we obtain the hadronic tensors:

$$\mathcal{A}_{H(^{2s+1}L_J)}^{\mu\nu} = \sqrt{\frac{2m_H\langle\mathcal{O}_1\rangle_L}{2N_c(2E)^2}}\mathcal{A}_Q^{\mu\nu(^{2s+1}L_J)}. \quad (13)$$

This step is equivalent to replacing the perturbative $Q\bar{Q}$ state $|[Q\bar{Q}]_1(^{2s+1}L_J)\rangle$ in Eq. (11) by the meson state $\sqrt{2m_H}|H(^{2s+1}L_J)\rangle$, where m_H is the mass of H . At leading order in v , $m_H = 2E|_{\mathbf{q}=0} = 2m$. The meson state $|H(^{2s+1}L_J)\rangle$, that is included in the vacuum-saturated analog of the NRQCD decay matrix elements $\langle\mathcal{O}_1\rangle_L$ for $L = S$ or P , has the nonrelativistic normalization:

$$|\langle H(^1S_0)|\psi^\dagger\chi|0\rangle|^2 = \langle\mathcal{O}_1\rangle_S, \quad (14a)$$

$$\frac{1}{3}|\langle H(^3P_0)|\psi^\dagger\left(-\frac{i}{2}\overleftrightarrow{\mathbf{D}}\cdot\boldsymbol{\sigma}\right)\chi|0\rangle|^2 = \langle\mathcal{O}_1\rangle_P, \quad (14b)$$

$$\frac{1}{2}|\langle H(^3P_1)|\psi^\dagger\left(-\frac{i}{2}\overleftrightarrow{\mathbf{D}}\times\boldsymbol{\sigma}\cdot\boldsymbol{\epsilon}_H\right)\chi|0\rangle|^2 = \langle\mathcal{O}_1\rangle_P, \quad (14c)$$

$$\left|\sum_{ij}\langle H(^3P_2)|\psi^\dagger\left(-\frac{i}{2}\overleftrightarrow{D}^{(i}\sigma^j)\epsilon_H^{ij}\right)\chi|0\rangle\right|^2 = \langle\mathcal{O}_1\rangle_P. \quad (14d)$$

The expressions in Eq. (14) have errors of relative order v^2 , which break the heavy-quark spin symmetry.

Substituting Eq. (11) into Eq. (13), we obtain the hadronic tensor $\mathcal{A}_H^{\mu\nu}$ in Eq. (1):

$$\mathcal{A}_{H(^1S_0)}^{\mu\nu} = -\frac{4e^2e_Q^2}{Q^2 - P^2} \epsilon^{\mu\nu\alpha\beta} P_\alpha Q_\beta \sqrt{\frac{\langle\mathcal{O}_1\rangle_S}{m}}, \quad (15a)$$

$$\mathcal{A}_{H(^3P_0)}^{\mu\nu} = i\frac{4e^2e_Q^2(Q^2 - 3P^2)}{\sqrt{3}(Q^2 - P^2)^2} \left[\frac{1}{2}(Q^2 - P^2)g^{\mu\nu} + P^\mu P^\nu \right] \sqrt{\frac{\langle\mathcal{O}_1\rangle_P}{m^3}}, \quad (15b)$$

$$\begin{aligned} \mathcal{A}_{H(^3P_1)}^{\mu\nu} &= \frac{4e^2e_Q^2Q^2\epsilon_{H\sigma}^*(\lambda_H)}{\sqrt{2}m(Q^2 - P^2)^2} \left[P^\mu P_\alpha Q_\beta \epsilon^{\nu\alpha\beta\sigma} - P^\nu P_\alpha Q_\beta \epsilon^{\mu\alpha\beta\sigma} - \frac{1}{2}(Q^2 - P^2)\epsilon^{\mu\nu\alpha\sigma} P_\alpha \right] \\ &\quad \times \sqrt{\frac{\langle\mathcal{O}_1\rangle_P}{m^3}}, \end{aligned} \quad (15c)$$

$$\begin{aligned} \mathcal{A}_{H(^3P_2)}^{\mu\nu} &= i\frac{8e^2e_Q^2P^2\epsilon_{H\alpha\beta}^*(\lambda_H)}{(Q^2 - P^2)^2} \left[g^{\mu\nu}Q^\alpha Q^\beta + P^\mu Q^\alpha g^{\nu\beta} - P^\nu Q^\alpha g^{\mu\beta} + \frac{1}{2}(Q^2 - P^2)g^{\mu\alpha}g^{\nu\beta} \right] \\ &\quad \times \sqrt{\frac{\langle\mathcal{O}_1\rangle_P}{m^3}}. \end{aligned} \quad (15d)$$

The hadronic tensor (15) can be compared with previous results for the color-octet processes $\gamma + g^* \rightarrow [Q\bar{Q}]_8(^{2s+1}L_J)$ [19]. We find that the results in Eq. (15) are consistent with those given in Eqs. (3.23), (3.25), (3.26), and (3.27) of Ref. [19] up to color factors. We have also checked that Eq. (15) reproduces the decay widths for η_Q , χ_{Q0} , and χ_{Q2} into two photons [4] in the limit $Q^2 \rightarrow 0$.

D. Cross section

Substituting the hadronic tensor $\mathcal{A}_H^{\mu\nu}$ in Eq. (15) and polarization states for the H and γ into Eq. (1), we obtain the helicity amplitude. By squaring the helicity amplitude, averaging over the spins of the e^+ and e^- , dividing by the incident flux $2s$, and multiplying by the two-body phase space, we obtain the differential cross section for each helicity state in terms of $x = \cos\theta$, where θ is the scattering angle of the photon at the CM frame. The resultant differential cross section for the $e^+e^- \rightarrow H(^1S_0) + \gamma$ process is

$$\frac{d\sigma}{dx}[e^+e^- \rightarrow H(^1S_0) + \gamma(\pm 1)] = \frac{\pi^2 e_Q^4 \alpha^3 r}{2s} \left(1 - \frac{m_H^2}{s}\right) (1+x^2) \frac{\langle\mathcal{O}_1\rangle_S}{m^3}, \quad (16)$$

where $-1 \leq x \leq 1$ and the scaling parameter r is defined by

$$r = \frac{4m^2}{s}. \quad (17)$$

The differential cross section of the $e^+e^- \rightarrow H(^3P_J) + \gamma$ process for each helicity state is given by

$$\frac{d\sigma}{dx}[e^+e^- \rightarrow H(^3P_J)(\lambda_H) + \gamma(\lambda)] = \frac{\pi^2 e_Q^4 \alpha^3 r}{s(1-r)^2} F_J(\lambda_H, \lambda) \left(1 - \frac{m_H^2}{s}\right) \frac{\langle \mathcal{O}_1 \rangle_P}{m^5}, \quad (18)$$

where nonvanishing entries of $F_J(\lambda_H, \lambda)$ are

$$F_0(0, \pm 1) = \frac{(1-3r)^2}{6}(1+x^2), \quad (19a)$$

$$F_1(0, \pm 1) = 1+x^2, \quad (19b)$$

$$F_1(\pm 1, \pm 1) = 2r(1-x^2), \quad (19c)$$

$$F_2(0, \pm 1) = \frac{1}{3}(1+x^2), \quad (19d)$$

$$F_2(\pm 1, \pm 1) = 2r(1-x^2), \quad (19e)$$

$$F_2(\pm 2, \pm 1) = 2r^2(1+x^2). \quad (19f)$$

In computing the phase space in Eqs. (16) and (18), we take the physical mass m_H instead of the invariant mass $2E$ of the $Q\bar{Q}$ pair. This accounts for the factor $1 - m_H^2/s$ in Eqs. (16) and (18).

When the CM energy \sqrt{s} is much greater than the heavy-quark mass m , the asymptotic behavior of the cross section for $e^+e^- \rightarrow H + \gamma$ satisfies the helicity selection rules of perturbative QCD [20, 21]. In this limit, the scaled cross section $R(H + \gamma)$ in units of the cross section for $\mu^+\mu^-$ approaches the asymptotic form [5]

$$R[H(\lambda_H) + \gamma] \sim \alpha v^{3+2n(L)} r^{1+|\lambda_H|}, \quad (20)$$

where $n(S) = 0$ and $n(P) = 1$. The factor $v^{3+2n(L)}$ in Eq. (20) arises from the wave function of the H . One power of r in Eq. (20) stems from the large momentum transfer which is required for the heavy-quark pair to form the heavy quarkonium with small relative momentum and the other powers arise from the helicity selection rules [5]. In the limit $r \rightarrow 0$, the differential cross sections in Eqs. (16) and (18) satisfy the asymptotic form (20). For the exclusive charmonium production associated with a photon at the B factories, the ratio $r \approx 0.07$ is small for $m_c = 1.4$ GeV. However, for the case of a bottomonium, $r \approx 0.76$ is of order 1 for $m_b = 4.6$ GeV. Therefore, the asymptotic behavior (20) is approximately satisfied only for the exclusive charmonium plus γ production at the B factories.

Integrating the differential cross section given in Eq. (16) over x and summing over the photon helicities, we find the total cross section for the process $e^+e^- \rightarrow H(^1S_0) + \gamma$:

$$\sigma[e^+e^- \rightarrow H(^1S_0) + \gamma] = \frac{8\pi^2 e_Q^4 \alpha^3 r}{3s} \left(1 - \frac{m_H^2}{s}\right) \frac{\langle \mathcal{O}_1 \rangle_S}{m^3}. \quad (21)$$

Integrating Eq. (18) over x and summing over the helicities of the photon and quarkonium, we obtain the total cross sections for $e^+e^- \rightarrow H(^3P_J) + \gamma$:

$$\sigma[e^+e^- \rightarrow H(^3P_0) + \gamma] = \frac{8\pi^2 e_Q^4 \alpha^3 r (1-3r)^2}{9s(1-r)^2} \left(1 - \frac{m_H^2}{s}\right) \frac{\langle \mathcal{O}_1 \rangle_P}{m^5}, \quad (22a)$$

$$\sigma[e^+e^- \rightarrow H(^3P_1) + \gamma] = \frac{16\pi^2 e_Q^4 \alpha^3 r (1+r)}{3s(1-r)^2} \left(1 - \frac{m_H^2}{s}\right) \frac{\langle \mathcal{O}_1 \rangle_P}{m^5}, \quad (22b)$$

$$\sigma[e^+e^- \rightarrow H(^3P_2) + \gamma] = \frac{16\pi^2 e_Q^4 \alpha^3 r (1+3r+6r^2)}{9s(1-r)^2} \left(1 - \frac{m_H^2}{s}\right) \frac{\langle \mathcal{O}_1 \rangle_P}{m^5}, \quad (22c)$$

where we have used the spin-1 and spin-2 polarization tensors for 3P_1 and 3P_2 states summed over polarization states:

$$\sum_{\lambda_H} \epsilon_H^\mu(\lambda_H) \epsilon_H^{*\alpha}(\lambda_H) = I^{\mu\alpha}, \quad (23a)$$

$$\sum_{\lambda_H} \epsilon_H^{\mu\nu}(\lambda_H) \epsilon_H^{*\alpha\beta}(\lambda_H) = \frac{1}{2}(I^{\mu\alpha} I^{\nu\beta} + I^{\mu\beta} I^{\nu\alpha}) - \frac{1}{3} I^{\mu\nu} I^{\alpha\beta}. \quad (23b)$$

III. PARAMETERS FOR THE NUMERICAL ANALYSIS

In order to predict the cross sections for $e^+e^- \rightarrow \eta_Q + \gamma$ and $\chi_{QJ} + \gamma$ at the B factories by using Eqs. (21) and (22), we need to determine the numerical values for the NRQCD matrix elements $\langle \mathcal{O}_1 \rangle_L$ and input parameters such as m , m_H , α , and α_s . In this section, we list the numerical values for those quantities that we use in this work.

A. Input parameters

The short-distance coefficients for the cross sections in Eqs. (21) and (22) depend on the heavy-quark mass m . We take the one-loop pole mass for the heavy-quark mass m : $m_c = 1.4 \pm 0.2$ GeV for the charm quark and $m_b = 4.6 \pm 0.1$ GeV for the bottom quark, respectively. As we mentioned earlier, we use the physical quarkonium mass for m_H in the phase-space factor $1 - m_H^2/s$ in Eqs. (21) and (22), where $m_{\eta_c} = 2.9804$ GeV, $m_{\eta_c(2S)} = 3.638$ GeV,

$m_{\chi_{c0}} = 3.41475$ GeV, $m_{\chi_{c1}} = 3.51066$ GeV, $m_{\chi_{c2}} = 3.55620$ GeV, $m_{\chi_{b0}} = 9.585944$ GeV, $m_{\chi_{b1}} = 9.89278$ GeV, and $m_{\chi_{b2}} = 9.991221$ GeV [22]. For the η_b mass, we take $m_{\eta_b} = 9.3889$ GeV [23].²

The cross sections in Eqs. (21) and (22) are proportional to α^3 . For the QED couplings α^2 for the virtual photon, we use the running coupling constant [24] $\alpha(\mu = \sqrt{s}) = 1/131$ at $\sqrt{s} = 10.58$ GeV. The QED coupling for the real photon is chosen to be $\alpha(\mu = z) \approx 1/132$, where $z = [(s - 2m^2)/2]^{1/2}$ is the invariant mass of the virtual heavy quark: $z \approx 7.3$ GeV and 5.9 GeV for the charmonium and the bottomonium, respectively.

B. Long-distance matrix elements

1. NRQCD matrix elements $\langle \mathcal{O}_1 \rangle_S$

The color-singlet NRQCD matrix elements for the S -wave spin-singlet charmonia, η_c and $\eta_c(2S)$, can be determined from the two-photon decay rates. However, up to errors of relative order v^2 that arise from the heavy-quark-spin-symmetry breaking, one can determine the values also by making use of the leptonic decay rates of the spin-triplet counterparts, which are far more accurately measured. Among various theoretical attempts to determine the matrix elements for the S -wave spin-singlet charmonia, we employ a recently developed method given in Refs. [14, 25, 26]. This method resums a class of relativistic corrections to the color-singlet contributions to the electromagnetic decay rates of both spin-singlet and triplet S -wave charmonia to all orders in v . The color-singlet NRQCD matrix element $\langle \mathcal{O}_1 \rangle_S$ for the η_c is taken to be $0.437_{-0.105}^{+0.111}$ GeV³ [26].

For the radially excited S -wave spin-singlet state $\eta_c(2S)$, the NRQCD matrix element determined from the measured decay width for $\eta_c(2S) \rightarrow \gamma\gamma$ differs significantly by about 4.6σ from that for $\psi(2S)$ determined from $\psi(2S) \rightarrow e^+e^-$. The difference is greater than the errors of neglecting spin-symmetry breaking effects. We suspect that the main reason for the discrepancy is originated from the assumption [27]:

$$\text{Br}[\eta_c(2S) \rightarrow K_S^0 K^\pm \pi^\mp] = \text{Br}[\eta_c \rightarrow K_S^0 K^\pm \pi^\mp]. \quad (24)$$

² Very recently, the BABAR Collaboration observed the η_b resonance in the photon energy spectrum in radiative $\Upsilon(3S)$ decay [23].

This assumption was imposed on the indirect determination of the partial width for $\eta_c(2S) \rightarrow \gamma\gamma$ from the measurement for $\gamma^*\gamma^* \rightarrow \eta_c(2S) \rightarrow K_S^0 K^\pm \pi^\mp$ [27]. In this work, instead of using this indirect determination of $\Gamma[\eta_c(2S) \rightarrow \gamma\gamma]$ in Ref. [27], we assume that the NRQCD matrix element determined from $\Gamma[\eta_c(2S) \rightarrow \gamma\gamma]$ must be the same as that determined from $\Gamma[\psi(2S) \rightarrow e^+e^-]$ within errors of relative order v^2 , which breaks the heavy-quark spin symmetry. Our assumption results in the prediction for the two-photon width of $\eta_c(2S)$: $\Gamma[\eta_c(2S) \rightarrow \gamma\gamma] = 2.92$ keV. Direct measurement of the two-photon width of $\eta_c(2S)$ may provide one with a stringent test of our assumption. We will present a detailed analysis regarding this point in a separate publication. Basic strategy for determining the matrix element is similar to that in Ref. [26]. Disregarding the assumption (24) and making use of the matrix element obtained from $\Gamma[\psi(2S) \rightarrow e^+e^-]$ based on the heavy-quark spin symmetry up to corrections of relative order v^2 , we find that $\langle \mathcal{O}_1 \rangle_S = 0.274_{-0.036}^{+0.042}$ GeV³ for $S = \eta_c(2S)$.

The NRQCD matrix element $\langle \mathcal{O}_1 \rangle_S$ for the η_b cannot be determined from $\eta_b \rightarrow \gamma\gamma$ because the measurement is not available, yet. Instead, we quote the value for the matrix element $\langle \mathcal{O}_1 \rangle_{\Upsilon(1S)}$ given in Eq. (23a) of Ref. [28], which is determined from $\Upsilon(1S) \rightarrow e^+e^-$. We assume that the heavy-quark spin symmetry is relatively well satisfied because $v^2 \sim 0.1$ is small for the bottomonium. The numerical value is $\langle \mathcal{O}_1 \rangle_S = 3.069_{-0.190}^{+0.207}$ GeV³ for $S = \eta_b$ [28].

2. NRQCD matrix elements $\langle \mathcal{O}_1 \rangle_P$

The generalization of the resummation of relativistic corrections [14] to the P -wave quarkonium has not been developed because of the complication due to the color-octet contributions. Therefore, for the spin-triplet P -wave charmonium χ_{cJ} , we determine the NRQCD matrix element $\langle \mathcal{O}_1 \rangle_P$ by comparing the v -leading NRQCD factorization formulas for the photonic decay widths [4]

$$\Gamma(\chi_{c0} \rightarrow \gamma\gamma) = 6\pi e_c^4 \alpha^2 m \left[1 + \frac{(3\pi^2 - 28)\alpha_s}{18\pi} \right]^2 \frac{\langle \mathcal{O}_1 \rangle_P}{m^5}, \quad (25a)$$

$$\Gamma(\chi_{c2} \rightarrow \gamma\gamma) = \frac{8\pi e_c^4 \alpha^2 m}{5} \left(1 - \frac{8\alpha_s}{3\pi} \right)^2 \frac{\langle \mathcal{O}_1 \rangle_P}{m^5} \quad (25b)$$

with corresponding measured values. The decay of χ_{c1} into $\gamma\gamma$ is absent due to Yang's theorem [29].

Substituting the numerical values $\text{Br}(\chi_{c0} \rightarrow \gamma\gamma) = (2.76 \pm 0.33) \times 10^{-4}$ [22], the total decay width $\Gamma_{\chi_{c0}} = 10.4 \pm 0.7$ MeV [22], $\alpha_s(\mu = m_{\chi_{cJ}}/2) = 0.32$, and $\alpha(\mu = m_{\chi_{cJ}}/2) = 1/133$ [24]

into Eq. (25a), we obtain $\langle \mathcal{O}_1 \rangle_P = \langle \mathcal{O}_1 \rangle_{\chi_{c0}}^{\gamma\gamma} = 0.051 \pm 0.010 \text{ GeV}^5$ for $P = \chi_{c0}$, where the superscript $\gamma\gamma$ indicates that the value is fit to the two-photon width. Taking into account $\text{Br}(\chi_{c2} \rightarrow \gamma\gamma) = (2.58 \pm 0.19) \times 10^{-4}$ [22] and $\Gamma_{\chi_{c2}} = 2.05 \pm 0.12 \text{ MeV}$ [22], we obtain the matrix element $\langle \mathcal{O}_1 \rangle_P = \langle \mathcal{O}_1 \rangle_{\chi_{c2}}^{\gamma\gamma} = 0.068 \pm 0.009 \text{ GeV}^5$ for $P = \chi_{c2}$. Here, the uncertainties from the heavy-quark mass are not included in both $\langle \mathcal{O}_1 \rangle_{\chi_{c0}}^{\gamma\gamma}$ and $\langle \mathcal{O}_1 \rangle_{\chi_{c2}}^{\gamma\gamma}$. In Ref. [5], the value $\langle \mathcal{O}_1 \rangle_{\chi_{c2}} = 0.053 \pm 0.009 \text{ GeV}^5$ was obtained by making use of a similar method. The main reason for the difference is the change in the measured branching fraction of the χ_{c2} decay into $\gamma\gamma$ from $(2.19 \pm 0.33) \times 10^{-4}$ [30] to $(2.58 \pm 0.19) \times 10^{-4}$ [22]. We take the weighted average over the spin states of χ_{c0} and χ_{c2} to determine $\langle \mathcal{O}_1 \rangle_P = 0.060_{-0.029}^{+0.043} \text{ GeV}^5$ for $P = \chi_{cJ}$, where the heavy-quark spin symmetry is imposed and the uncertainty from the heavy-quark mass is considered together with those from the experimental values.

In the cases of the spin-triplet P -wave bottomonium states $\chi_{bJ}(1P)$, the measured values for the two-photon decay widths are not available. Therefore, we use the first derivative of the wave function at the origin that has been determined by using the Buchmüller-Tye potential [31]. The resultant value for the NRQCD matrix element is $\langle \mathcal{O}_1 \rangle_P = 2.03 \text{ GeV}^5$ for $P = \chi_{bJ}$ [32].

3. Summary of NRQCD matrix elements

In Table I, we tabulate the color-singlet NRQCD matrix elements for η_c , $\eta_c(2S)$, η_b , χ_{cJ} , and χ_{bJ} . As has been described in the text, there are input parameters such as m that have been used to determine the NRQCD matrix elements. When we compute the short-distance coefficients for the cross section for $e^+e^- \rightarrow H + \gamma$, such input parameters must be consistent with the values that have been used to determine the NRQCD matrix elements [26]. In order to take into account such correlations, we present sources of the uncertainties for each NRQCD matrix element in Table I. The first and the second lines after headings contain uncertainties arising from the heavy-quark mass m and from sources described in each reference except for m , respectively. The sum of the two uncertainties is obtained by adding them in quadrature as shown in the last row of Table I.

TABLE I: NRQCD matrix elements $\langle \mathcal{O}_1 \rangle_H$ for $H(^1S_0)$ in units of GeV^3 and for $H(^3P_J)$ in units of GeV^5 . The first and the second lines after headings contain uncertainties arising from the heavy-quark mass m and from other sources described in the text. Uncertainties in the last line are obtained by adding the two uncertainties in quadrature.

Sources of errors \ H	η_c [26] (GeV^3)	$\eta_c(2S)$ (GeV^3)	η_b [32] (GeV^3)	χ_{cJ} (GeV^5)	χ_{bJ} [31, 32] (GeV^5)
Δm	$0.437^{+0.033}_{-0.025}$	$0.274^{+0.013}_{-0.010}$	$3.069^{+0.000}_{-0.000}$	$0.060^{+0.043}_{-0.028}$	2.03
others	$0.437^{+0.106}_{-0.102}$	$0.274^{+0.040}_{-0.035}$	$3.069^{+0.207}_{-0.190}$	0.060 ± 0.007	2.03
total	$0.437^{+0.111}_{-0.105}$	$0.274^{+0.042}_{-0.036}$	$3.069^{+0.207}_{-0.190}$	$0.060^{+0.043}_{-0.029}$	2.03

IV. PREDICTIONS FOR THE B FACTORIES

In this section, we provide the predictions for the cross sections for $e^+e^- \rightarrow H + \gamma$ at the B factories. We also discuss the uncertainties and phenomenological implications of the results.

Our predictions for the total cross section σ for $e^+e^- \rightarrow H + \gamma$ at the CM energy $\sqrt{s} = 10.58 \text{ GeV}$ are given in the first column of Table II. The values have been obtained by substituting the input parameters listed in Sec. III into the NRQCD factorization formulas in Eqs. (21) and (22). In the second column, we provide the cross section σ_{cut} in which we have imposed the cut $|\cos\theta| < 0.8$ for the scattering angle θ of the photon at the CM frame. σ_{cut} is about 70%–80% of σ in any case. In the last column in Table II, we list the energy $E_\gamma = (s - m_H^2)/(2\sqrt{s})$ of the photon emitted in $e^+e^- \rightarrow H + \gamma$ at the CM frame, which may provide an efficient trigger for the signals.

A. Uncertainties

The error bars of the cross sections σ and σ_{cut} listed in Table II contain the following uncertainties. A dominant source of the uncertainties is the heavy-quark mass m , which affects both the NRQCD matrix elements in Table I and the short-distance coefficients appearing in the NRQCD factorization formulas in Eqs. (21) and (22). To avoid double counting of those errors, we have considered the correlation of the uncertainties from m .

TABLE II: The total cross section σ in units of fb and the photon energy E_γ at the CM frame in units of GeV in $e^+e^- \rightarrow H + \gamma$ depending on charge-conjugation parity $C = +1$ quarkonium H . The subscript “cut” represents the cut $|\cos \theta| < 0.8$ for the scattering angle θ of the photon at the CM frame.

H	σ (fb)	σ_{cut} (fb)	E_γ (GeV)
η_c	$82.0^{+21.4}_{-19.8}$	$59.7^{+15.6}_{-14.4}$	4.87
$\eta_c(2S)$	$49.2^{+9.4}_{-7.4}$	$35.8^{+6.8}_{-5.4}$	4.66
η_b	$2.5^{+0.2}_{-0.2}$	$1.8^{+0.1}_{-0.1}$	1.12
χ_{c0}	$1.3^{+0.2}_{-0.2}$	$1.0^{+0.1}_{-0.1}$	4.74
χ_{c1}	$13.7^{+3.4}_{-3.1}$	$10.2^{+2.6}_{-2.3}$	4.71
χ_{c2}	$5.3^{+1.6}_{-1.3}$	$4.0^{+1.3}_{-1.0}$	4.69
χ_{b0}	$0.6^{+0.3}_{-0.2}$	$0.4^{+0.2}_{-0.1}$	0.95
χ_{b1}	$2.8^{+0.8}_{-0.5}$	$2.3^{+0.6}_{-0.4}$	0.66
χ_{b2}	$3.0^{+1.0}_{-0.7}$	$2.4^{+0.8}_{-0.5}$	0.57

Other errors in $\langle \mathcal{O}_1 \rangle_S$ include a theoretical uncertainty of relative order v^2 from the leading-potential approximation, the uncertainty of the string tension, which is a parameter of the Cornell potential model, the uncertainty reflecting the uncalculated next-to-next-to-leading-order corrections in α_s to the electromagnetic decay width of the quarkonium, and the uncertainty of the measured decay width. For more details about the error analysis, we refer the reader to Refs. [26]. The error bars of the NRQCD matrix elements $\langle \mathcal{O}_1 \rangle_P$ for the χ_{cJ} in Table I include the uncertainties from the heavy-quark mass m and the measured widths for the two-photon decays of the χ_{c0} and χ_{c2} . The NRQCD matrix elements $\langle \mathcal{O}_1 \rangle_P$ for the χ_{bJ} are quoted from Refs. [31, 32], where uncertainties are not included [32]. As a result, except for the uncertainties from the heavy-quark mass m appearing in the short-distance coefficients, no additional uncertainties are included in the error bars of the cross section for $H = \chi_{bJ}$. The error bars of σ and σ_{cut} in Table II have been obtained by adding all the uncertainties listed above in quadrature.

Our predictions in Table II may suffer from QCD and relativistic corrections that have not been calculated, yet. We guess that the corrections may not be as large as those observed in the two-charmonium production from e^+e^- annihilation [12, 15, 16, 33], where all such

corrections are aligned to make a significant enhancement of the prediction for the cross section.

B. Exclusive $\eta_c(1S, 2S) + \gamma$ production

As we have shown in Table II, the cross sections for the S -wave spin-singlet charmonia $H = \eta_c$ and $\eta_c(2S)$ produced exclusively with a photon are about 80 fb and about 50 fb, respectively. These values are significantly greater than those for $J/\psi + \eta_c$ and $J/\psi + \eta_c(2S)$ measured at the B factories. We have predicted that $\Gamma[\eta_c(2S) \rightarrow \gamma\gamma] = 2.92$ keV by replacing the assumption (24) that was imposed on the indirect determination of $\Gamma[\eta_c(2S) \rightarrow \gamma\gamma]$ in Refs. [34, 35] with an alternative assumption that the approximate heavy-quark spin symmetry still holds between the NRQCD matrix elements for $\eta_c(2S)$ and $\psi(2S)$. The measurement of the cross section for $e^+e^- \rightarrow \eta_c(2S) + \gamma$ is particularly interesting because the measurement may provide an independent test of our argument presented in Sec. III B 1.

C. Exclusive $\eta_b + \gamma$ production

Our prediction of the cross section for $H = \eta_b$ at the B factories is about 2.5 fb. By taking into account the integrated luminosities available at the present B factories, we expect that over three thousands of $e^+e^- \rightarrow \eta_b + \gamma$ events can be produced. This number exceeds the estimated number of events at LEP II through $\gamma^*\gamma^* \rightarrow \eta_b$ by about an order of magnitude [36–38]. Therefore, the exclusive process $e^+e^- \rightarrow \eta_b + \gamma$ could be an alternative probe to the η_b meson as long as the background can be removed significantly.

D. Exclusive $\chi_{QJ} + \gamma$ production

As shown in Table II, the cross section for $H = \chi_{QJ}$ ranges from about 1 to 5 fb except for the case of χ_{c1} , which has a particularly large value of about 14 fb. The reason is that the overall coefficient for the longitudinal χ_{Q1} is greater than those for the other two states as shown in Eq. (19).³ This contrasts to the P -wave decay into $\gamma\gamma$, where $\chi_{Q1} \rightarrow \gamma\gamma$ is forbidden by Yang's theorem [29]. A similar feature can be found in the inclusive charm

³ According to the hadron helicity selection rules, the longitudinal cross section for χ_{QJ} dominates as $r \rightarrow 0$.

production in χ_{bJ} decay [32]: the decay rate of the χ_{b1} into g^*g is comparable to those of the χ_{b0} and the χ_{b2} , especially in the limit of the large invariant mass of the g^* . Unlike the P -wave spin-triplet charmonium, the cross sections for χ_{b1} and χ_{b2} are comparable and that for χ_{b0} is much suppressed.

E. Backgrounds

The exclusive process $e^+e^- \rightarrow H + \gamma$ for $C = +1$ heavy quarkonium H suffers from large contamination from the background $e^+e^- \rightarrow X + \gamma$. In this section, we provide a rough estimate on the background.

We assume that the dominant subprocesses of the background $e^+e^- \rightarrow X + \gamma$ are $e^+e^- \rightarrow q\bar{q} + \gamma$, where $q = u, d, s$, and c . These processes have collinear divergences due to the photon radiation from the initial leptons and final massless quarks. In order to avoid such complications, we take the following cuts: $|\cos\theta| < 0.8$, $\cos\theta_{q\gamma} < 0.8$, and $\cos\theta_{\bar{q}\gamma} < 0.8$, where θ is the scattering angle of the photon and $\theta_{i\gamma}$ is the relative angle between the photon and a quark or an antiquark i in the CM frame. We also restrict the energy range of the photon by requiring the recoil mass m_X to satisfy $|m_X - m_H| < 50$ MeV.

By imposing the constraints listed above, we carry out the numerical calculation for the background cross section $\sigma_{\text{BG}}(H)$ for each $C = +1$ heavy quarkonium H by making use of CompHEP [39]. The results are $\sigma_{\text{BG}}(\text{charmonium}) \approx 0.5$ pb and $\sigma_{\text{BG}}(\text{bottomonium}) \approx 2.4$ – 4.5 pb. The background cross sections $\sigma_{\text{BG}}(H)$ are much greater than the signal cross sections σ_{cut} in Table II. However, the high integrated luminosities \mathcal{L} of order 1 ab^{-1} of the present B factories might allow one to measure the exclusive $C = +1$ quarkonium production associated with a photon. We can compute the signal significance $S(H)$ for each heavy quarkonium, where $S(H)$ is defined by

$$S(H) = \frac{\sigma_{\text{cut}}(H + \gamma)\mathcal{L}}{\sqrt{\sigma_{\text{BG}}(H)\mathcal{L}}}. \quad (26)$$

We find that S -wave charmonium states have particularly large values: $S(\eta_c) \approx 81$ and $S[\eta_c(2S)] \approx 47$. In the cases of P -wave charmonium states, $S(\chi_{c0}) \approx 1$, $S(\chi_{c1}) \approx 13$, and $S(\chi_{c2}) \approx 5$. And $S(H)$ is less than 1 for η_b and χ_{bJ} states.

Our background study given above is only a rough estimate. In the cases of bottomonium states, there must be obstacles in detecting photons with energies about 1 GeV or

less because of the large contamination from the decays of light hadrons [40]. However, the exclusive charmonium production associated with a photon may have significantly less additional backgrounds unlike the bottomonium states because the radiating photon is sufficiently hard. We also note that there may be another background arising from the feeddown from the $e^+e^- \rightarrow H(^3S_1) + \gamma$ process for $H(^3S_1) = J/\psi, \psi(2S)$, or $\Upsilon(nS)$, whose cross sections are of order pb. Especially, the measurement of the $\chi_{QJ} + \gamma$ production may be affected by such feeddown. Reduction of such backgrounds may be subject to detector resolution.

V. SUMMARY

We have calculated the cross section for the $C = +1$ heavy quarkonium H produced exclusively with a photon from e^+e^- annihilation into a virtual photon at leading order in α_s and v . The NRQCD factorization formulas for the differential distributions with respect to the scattering angle of the photon and the total cross sections for $H = \eta_Q$ and χ_{QJ} have been obtained in Eqs. (16), (18), (21), and (22), respectively. Our predictions for the cross sections at $\sqrt{s} = 10.58$ GeV are tabulated in Table II. The predicted cross sections for the S -wave spin-singlet states are about 80 fb, 50 fb, and 3 fb for $\eta_c, \eta_c(2S)$, and η_b , respectively. In the cases of the P -wave spin-triplet charmonia, the cross section for χ_{c1} is about 14 fb; that is significantly greater than those for χ_{c0} and χ_{c2} . The cross sections for χ_{b1} and χ_{b2} are about 3 fb and that for χ_{b0} is suppressed. Under the cut $|\cos\theta| < 0.8$ for the scattering angle θ of the photon, the cross sections decrease by about 20%–30 %.

The exclusive process $e^+e^- \rightarrow H + \gamma$ may suffer from a large background from $e^+e^- \rightarrow X + \gamma$. A rough estimate on the background cross section has been made by considering only the $e^+e^- \rightarrow q\bar{q} + \gamma$ contributions at leading order in α_s . In computing the background cross section, we have required $|m_X - m_H| < 50$ MeV for the recoil mass m_X and imposed the angular cuts $|\cos\theta| < 0.8$, $\cos\theta_{q\gamma} < 0.8$, and $\cos\theta_{\bar{q}\gamma} < 0.8$. The resultant background cross sections are about 0.5 pb for the charmonia and about several pb for the bottomonia. The signal significances for the $\eta_c, \eta_c(2S), \chi_{c1}$, and χ_{c2} cases are greater than 6. However, those for the η_b, χ_{c0} , and χ_{bJ} are about 1 at the present B factories.

Very recently, the BABAR Collaboration observed the η_b resonance in the photon energy spectrum in radiative $\Upsilon(3S)$ decay [23]. The exclusive process $e^+e^- \rightarrow \eta_b + \gamma$ that we have considered could be an alternative probe to the η_b meson as long as the backgrounds are

significantly removed.

As we have remarked earlier, the authors of Refs. [34] and [35] made an assumption $\text{Br}[\eta_c(2S) \rightarrow K_S^0 K^\pm \pi^\mp] = \text{Br}[\eta_c \rightarrow K_S^0 K^\pm \pi^\mp]$ in determining the $\Gamma[\eta_c(2S) \rightarrow \gamma\gamma] = 1.3 \pm 0.6$ keV [34] and 0.59 ± 0.19 keV [35], respectively. This assumption seems to be the origin of inconsistency of the NRQCD matrix element for $\eta_c(2S)$, which was fit to $\Gamma[\eta_c(2S) \rightarrow \gamma\gamma]$ [34, 35], in comparison with that for $\psi(2S)$. As an alternative choice, we assume that the approximate heavy-quark spin symmetry holds between the NRQCD matrix elements for the $\eta_c(2S)$ and $\psi(2S)$ to predict $\Gamma[\eta_c(2S) \rightarrow \gamma\gamma] = 2.92$ keV. The measurement of the cross sections for $e^+e^- \rightarrow \eta_c + \gamma$ and $e^+e^- \rightarrow \eta_c(2S) + \gamma$ may provide a stringent independent constraint to test our argument.

Acknowledgments

We thank Sadaharu Uehara and Eunil Won for critical comments and useful discussions. The work of HSC was supported by the BK21 program. The work of JL was supported by the Korea Science and Engineering Foundation (KOSEF) funded by the Korea government (MEST) under Grant No. R01-2008-000-10378-0. The work of CY was supported by the Korea Research Foundation Grant funded by the Korean Government (MOEHRD, Basic Research Promotion Fund) (KRF-2006-311-C00020).

-
- [1] K. Abe *et al.* [Belle Collaboration], Phys. Rev. Lett. **89**, 142001 (2002) [arXiv:hep-ex/0205104].
 - [2] K. Abe *et al.* [Belle Collaboration], Phys. Rev. D **70**, 071102 (2004) [arXiv:hep-ex/0407009].
 - [3] B. Aubert *et al.* [BABAR Collaboration], Phys. Rev. D **72**, 031101 (2005) [arXiv:hep-ex/0506062].
 - [4] G. T. Bodwin, E. Braaten, and G. P. Lepage, Phys. Rev. D **51**, 1125 (1995) [Erratum-ibid. D **55**, 5853 (1997)] [arXiv:hep-ph/9407339].
 - [5] E. Braaten and J. Lee, Phys. Rev. D **67**, 054007 (2003) [Erratum-ibid. D **72**, 099901 (2005)] [arXiv:hep-ph/0211085].
 - [6] K. Y. Liu, Z. G. He, and K. T. Chao, Phys. Lett. B **557**, 45 (2003) [arXiv:hep-ph/0211181].
 - [7] G. T. Bodwin, J. Lee, and E. Braaten, Phys. Rev. Lett. **90**, 162001 (2003) [arXiv:hep-

- ph/0212181].
- [8] G. T. Bodwin, J. Lee, and E. Braaten, Phys. Rev. D **67**, 054023 (2003) [Erratum-ibid. D **72**, 099904 (2005)] [arXiv:hep-ph/0212352].
 - [9] S. J. Brodsky, A. S. Goldhaber, and J. Lee, Phys. Rev. Lett. **91**, 112001 (2003) [arXiv:hep-ph/0305269].
 - [10] A. E. Bondar and V. L. Chernyak, Phys. Lett. B **612**, 215 (2005) [arXiv:hep-ph/0412335].
 - [11] G. T. Bodwin, D. Kang, and J. Lee, Phys. Rev. D **74**, 114028 (2006) [arXiv:hep-ph/0603185].
 - [12] Y. J. Zhang, Y. j. Gao, and K. T. Chao, Phys. Rev. Lett. **96**, 092001 (2006) [arXiv:hep-ph/0506076].
 - [13] B. Gong and J. X. Wang, Phys. Rev. D **77**, 054028 (2008) [arXiv:0712.4220 [hep-ph]].
 - [14] G. T. Bodwin, D. Kang, and J. Lee, Phys. Rev. D **74**, 014014 (2006) [arXiv:hep-ph/0603186].
 - [15] G. T. Bodwin, D. Kang, T. Kim, J. Lee, and C. Yu, AIP Conf. Proc. **892**, 315 (2007) [arXiv:hep-ph/0611002].
 - [16] G. T. Bodwin, J. Lee, and C. Yu, Phys. Rev. D **77**, 094018 (2008) [arXiv:0710.0995 [hep-ph]].
 - [17] G. T. Bodwin, X. Garcia i Tormo, and J. Lee, Phys. Rev. Lett. **101**, 102002 (2008) [arXiv:0805.3876 [hep-ph]].
 - [18] G. T. Bodwin and A. Petrelli, Phys. Rev. D **66**, 094011 (2002) [arXiv:hep-ph/0205210].
 - [19] P. Ko, J. Lee, and H. S. Song, Phys. Rev. D **54**, 4312 (1996) [Erratum-ibid. D **60**, 119902 (1999)] [arXiv:hep-ph/9602223].
 - [20] V. L. Chernyak and A. R. Zhitnitsky, Sov. J. Nucl. Phys. **31**, 544 (1980) [Yad. Fiz. **31**, 1053 (1980)].
 - [21] S. J. Brodsky and G. P. Lepage, Phys. Rev. D **24**, 2848 (1981).
 - [22] W. M. Yao *et al.* [Particle Data Group], J. Phys. G **33**, 1 (2006).
 - [23] B. Aubert *et al.* [BABAR Collaboration], arXiv:0807.1086 [hep-ex].
 - [24] For numerical values for α and α_s , we make use of the code GLOBAL ANALYSIS OF PARTICLE PROPERTIES (GAPP). For details, refer to the following references; J. Erler, Phys. Rev. D **59**, 054008 (1999) [arXiv:hep-ph/9803453]; arXiv:hep-ph/0005084.
 - [25] H. S. Chung, J. Lee, and D. Kang, J. Korean Phys. Soc. **52**, 1151 (2008) [arXiv:0803.3116 [hep-ph]].
 - [26] G. T. Bodwin, H. S. Chung, D. Kang, J. Lee, and C. Yu, Phys. Rev. D **77**, 094017 (2008) [arXiv:0710.0994 [hep-ph]].

- [27] S. B. Athar *et al.* [CLEO Collaboration], Phys. Rev. D **70**, 112002 (2004) [arXiv:hep-ex/0408133].
- [28] D. Kang, T. Kim, J. Lee, and C. Yu, Phys. Rev. D **76**, 114018 (2007) [arXiv:0707.4056 [hep-ph]].
- [29] C. N. Yang, Phys. Rev. **77**, 242 (1950).
- [30] K. Hagiwara *et al.* [Particle Data Group], Phys. Rev. D **66**, 010001 (2002).
- [31] E. J. Eichten and C. Quigg, Phys. Rev. D **52**, 1726 (1995) [arXiv:hep-ph/9503356].
- [32] G. T. Bodwin, E. Braaten, D. Kang, and J. Lee, Phys. Rev. D **76**, 054001 (2007) [arXiv:0704.2599 [hep-ph]].
- [33] Z. G. He, Y. Fan, and K. T. Chao, Phys. Rev. D **75**, 074011 (2007) [arXiv:hep-ph/0702239].
- [34] D. M. Asner *et al.* [CLEO Collaboration], Phys. Rev. Lett. **92**, 142001 (2004) [arXiv:hep-ex/0312058].
- [35] S. Eidelman, Talk given at International Workshop on Heavy Quarkonium 2007 (QWG 2007), DESY, Hamburg, 17-20 Oct 2007.
- [36] A. Heister *et al.* [ALEPH Collaboration], Phys. Lett. B **530**, 56 (2002) [arXiv:hep-ex/0202011].
- [37] M. Levtchenko [L3 Collaboration], Nucl. Phys. Proc. Suppl. **126**, 260 (2004).
- [38] A. Sokolov, Nucl. Phys. Proc. Suppl. **126**, 266 (2004).
- [39] E. Boos *et al.* [CompHEP Collaboration], Nucl. Instrum. Meth. A **534**, 250 (2004) [arXiv:hep-ph/0403113].
- [40] Sadaharu Uehara, private communication.